

Noise in disordered systems: The power spectrum and dynamic exponents in avalanche models

Matthew C. Kuntz* and James P. Sethna†

LASSP, Department of Physics, Cornell University, Ithaca, NY 14853

(Dated: May 19, 2019)

For a long time, it has been known that the power spectrum of Barkhausen noise had a power-law decay at high frequencies. Up to now, the theoretical predictions for this decay have been incorrect, or have only applied to a small set of models. In this paper, I describe a careful derivation of the power spectrum exponent in avalanche models, and in particular, in variations of the zero-temperature random-field Ising model. I find that the naive exponent, $(3 - \tau)/\sigma\nu z$, which has been derived in several other papers, is in general incorrect for small τ , when large avalanches are common. (τ is the exponent describing the distribution of avalanche sizes, and $\sigma\nu z$ is the exponent describing the relationship between avalanche size and avalanche duration.) I find that for a large class of avalanche models, including several models of Barkhausen noise, the correct exponent for $\tau < 2$ is $1/\sigma\nu z$. I also explicitly derive the mean-field exponent of 2.

I. INTRODUCTION

Many physical systems, from super-conductors¹ to sandpiles² to martensitic shape-memory alloys³ produce noise with power law characteristics. The noise in many of these systems can be modeled in terms of avalanches. One example of this is Barkhausen noise in ferromagnetic materials. Many ferromagnetic materials magnetize not smoothly, but in jumps of all sizes. The resulting “noise” is characterized by power laws. For example, the distributions of avalanche sizes, durations and energies are all seen to be power laws. Recently, it has been proposed that this noise is a result of either a disorder induced critical point^{4,5,6,7,8,9}, or self organized criticality (SOC)^{10,11}. Several variations of the zero temperature random field Ising model have been proposed to model this critical behavior.

One of the main power laws which must be explained if these models are to be successful is the power law behavior of the power spectrum. Actually, the power spectrum exhibits two different power laws, one for low frequencies, and another for high frequencies. The high frequency power law, $\mathcal{P}_{\text{av}}(\omega)$, reflects the dynamics within avalanches, and the low frequency power law, $\mathcal{P}_{\text{corr}}(\omega)$, reflects the correlations between avalanches. Simulations of various random field Ising models have been fairly successful in modeling the high frequency scaling of the power spectrum, but theoretical predictions of this scaling have been absent or wrong.^{5,8,9,12} (See the discussion in section V for a description of several previous calculations.) In this paper, I will derive an exponent relation for the high frequency power spectrum which applies to several variations of the random-field Ising model. Large portions of the derivation should also apply to any critical avalanche model.

II. THE MODELS

Several variations of the zero temperature random field Ising model have been proposed to explain the power laws in Barkhausen noise. They are differentiated on the basis of the presence of long range forces, and the details of the dynamics. In a separate paper, we examine in detail the differences between these models¹³. A general Hamiltonian for the models is

$$\begin{aligned} \mathcal{H} = & - \sum_{\text{nn}} J_{\text{nn}} s_i s_j - \sum_i H s_i - \sum_i h_i s_i \\ & + \sum_i \frac{J_{\text{inf}}}{N} s_i - \sum_{\{i,j\}} J_{\text{dipole}} \frac{3 \cos(\theta_{ij}) - 1}{r_{ij}^3} s_i s_j, \end{aligned} \quad (1)$$

where s_i is an Ising spin $s_i = \pm 1$, J_{nn} is the strength of the ferromagnetic nearest neighbor interactions, H is an external magnetic field, h_i is a random local field, J_{inf} is the strength of the infinite range demagnetizing field, and J_{dipole} is the strength of the dipole-dipole interactions. The power laws are independent of the particular choice of random field distributions $\rho(h_i)$ for a large variety of distributions. Most commonly, a Gaussian distribution of random fields is used, with a standard deviation R . (When I refer to the strength of the disorder, I am referring to the width, R , of the random field distribution.)

Two different dynamics have been considered. The first is a front propagation dynamics in which spins on the edge of an existing front flip as soon as it would decrease their energy to do so. Spins with no flipped neighbors cannot flip

	Short Range (3D)	Front Propagation (3D)	Mean Field
τ	1.6	1.28	1.5
$\sigma\nu z$	0.58	0.58	0.5
Short Range (4D) Front Propagation (4D)			
τ	1.53	1.42	
$\sigma\nu z$	0.52	0.56	

TABLE I: Important exponents for the three universality classes. τ is the exponent for the avalanche size distribution $D(S) = S^{-\tau}$. $\sigma\nu z$ relates the avalanche size S to the avalanche duration T : $T \sim S^{\sigma\nu z}$

even if it would be energetically favorable. Second is a dynamics which includes domain nucleation. Any spin can flip when it becomes energetically favorable to do so. In both cases, spins flip in shells—all spins which can flip at time t flip, then all of their newly flippable neighbors flip at time $t + 1$.

Depending on which terms are included in the Hamiltonian, the behavior appears to fall into three different universality classes. When domain nucleation is allowed, and only nearest neighbor interactions are included, there is a second order critical point at a particular disorder, R_c , and external field H_c . For disorders below R_c , a finite fraction of the spins in the system (even in the thermodynamic limit) flip in a single jump. This critical point seems to have a wide critical region,^{4,5,6,7,8,9} so this critical behavior might be seen in experiments even without tuning the disorder. For disorders below R_c , or when domain nucleation is not allowed, the addition of an infinite-range demagnetizing field²⁰ can self-organize the system to a different critical behavior. (Self-organization means that the system naturally sits at a critical point, without having to tune any parameters.) This critical behavior was originally described in a non-self-organized depinning model by Ji and Robbins.^{14,21} Zapperi *et al.* and Narayan^{11,15} claim that the addition of dipole-dipole interactions to the infinite-range model lowers the upper critical dimension to three and produces mean-field exponents in three dimensions. Since large mean-field simulations are much easier than large simulations with dipole-dipole interactions, we will give results from mean-field simulations in this paper. The relevant exponents for the three universality classes can be found in table I. Except in section IV, all of the results in this paper are from three-dimensional simulations with nearest neighbor and infinite range interactions, which exhibit self-organized front-propagation exponents.

III. DERIVING THE EXPONENTS

In the process of deriving the form of the critical exponent for the energy spectrum, we will derive the scaling forms of several other quantities which are themselves of interest. Warned by the failure of the naive scaling exponent for the energy spectrum, we will present numerical scaling plots for each of these intermediate quantities.

A. The avalanche shape

Near criticality, the avalanches in the random-field Ising model have a very ragged shape. There are avalanches of all sizes precisely because each avalanche is always finely balanced between continuing and dying out. Most large avalanches come close to dying many times. A typical large avalanche can be seen in figure 1.

Despite this rough shape, criticality implies that the average avalanche shape will scale in a universal way. Consider the average shape of avalanches of duration T . If we rescale the time axis, t , by a factor of T , and divide the vertical axis, which measures the number of spins flipped (or the voltage V which would be measured in a pickup coil), by the average voltage, we should get a generic shape which is independent of T . The average height is the average area, $S(T) \sim T^{1/\sigma\nu z}$ (let this define the exponent $\sigma\nu z$)²², divided by the duration, T . Therefore, the scaling form should be

$$V(T, t) = T^{1/\sigma\nu z - 1} f(t/T). \quad (2)$$

The scaling of the average avalanche shape according to equation 2 can be seen in figure 2.²³

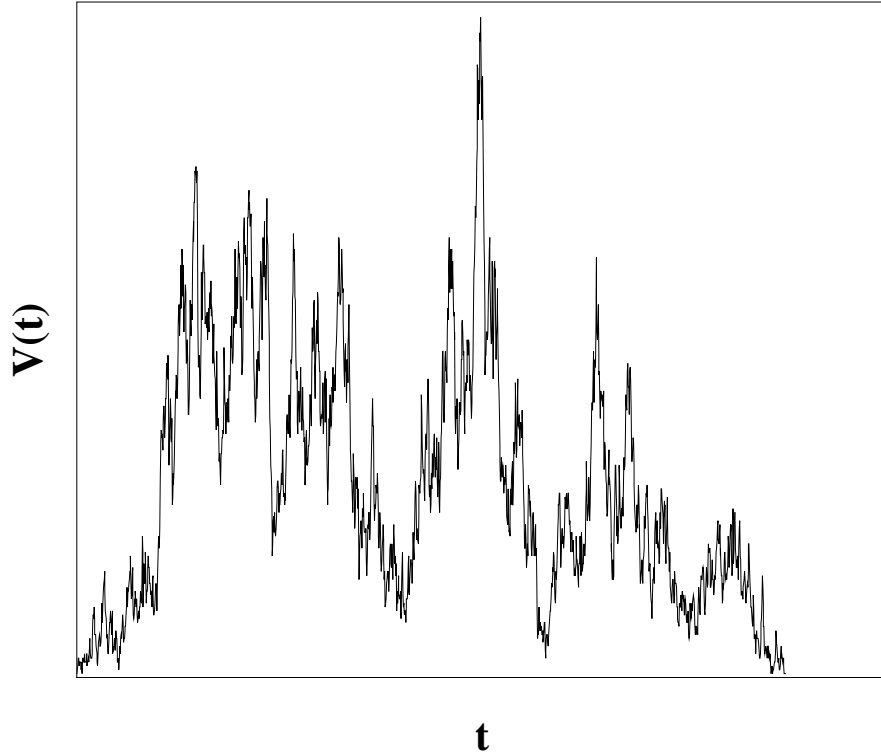


FIG. 1: The shape of a typical large avalanche. Notice that the avalanche nearly stopped several times, and the voltage (the number of spins flipped in each time step) fluctuated drastically.

B. Distribution of voltages V in avalanches of size S

The power spectrum is sensitive not only to the shapes of the avalanches, but to the fluctuations in the avalanche shapes. An interesting measure of these fluctuations is the probability $P(V|S)$ that a voltage V will occur at some point in an avalanche of size S . If this probability scales universally, then we know it must have the form

$$P(V|S) = V^{-x} f(VS^{-y}). \quad (3)$$

But what are the exponents x and y ? We can determine the value of x by integrating over all voltages. Since $P(V|S)$ is a probability distribution, it must integrate to 1:

$$\int_0^\infty V^{-x} f(VS^{-y}) dV = AS^{-y(x-1)} = 1. \quad (4)$$

From this, we know that $x = 1$. (The alternative, $y = 0$, can be discarded because along with equation 3 it would imply that $P(V|S)$ is independent of the avalanche size S .)

We also know that the average voltage in the avalanche must be equal to the avalanche size S divided by the avalanche duration $T \sim S^{\sigma\nu z}$, so

$$\begin{aligned} \langle V \rangle &= \int_0^\infty V P(V|S) dV \\ &= \int_0^\infty f(VS^{-y}) dV \\ &= S^y = S^{1-\sigma\nu z}. \end{aligned} \quad (5)$$

From this, we know that $y = 1 - \sigma\nu z$, and the probability of a voltage V occurring in an avalanche of size S is

$$P(V|S) = V^{-1} f(VS^{\sigma\nu z-1}). \quad (6)$$

As can be seen in figure 3, this scaling form works very well.

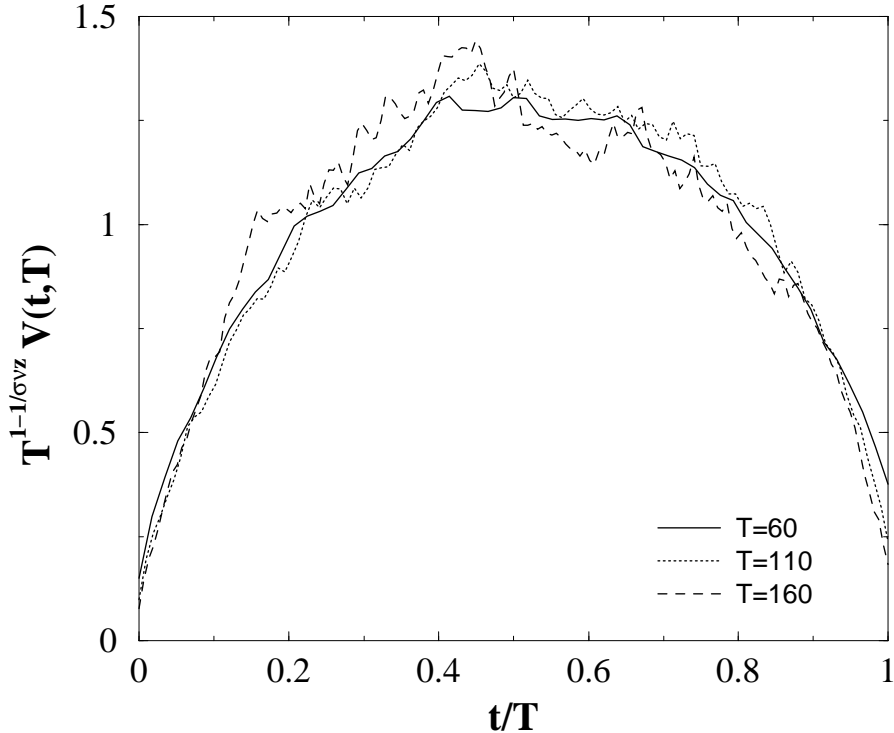


FIG. 2: The average avalanche shape for three different durations. Spasojević *et al.*¹² measured the average avalanche shape experimentally and found a somewhat different shape. This kind of measurement provides a much sharper test for the theory than the tradition of comparing critical exponents. Presumably, the average avalanche shape for large sizes and times is a universal scaling function: if the experiment differs in this regard from our model, then our model is expected to have different critical exponents. All features at long length and time scales should be universal.

C. The scaling of avalanche energy E with avalanche size S

The voltage distribution in equation 6 allows us to calculate the dependence of avalanche energy on avalanche size. The avalanche energy is simply the average squared voltage, $\langle V^2 \rangle$, times the average avalanche duration, $S^{\sigma\nu z}$. Using equation 6, this is

$$\begin{aligned}
 E(S) &= S^{\sigma\nu z} \int_0^\infty V^2 P(V|S) dV \\
 &= S^{\sigma\nu z} \int_0^\infty V f(V S^{\sigma\nu z - 1}) dV \\
 &= S^{2 - \sigma\nu z}.
 \end{aligned} \tag{7}$$

Note that this is the same result we would find if we assumed that the time dependence had a square profile.

D. The scaling of the time-time correlation function with S

With this information, we can calculate the scaling of the time-time correlation function within avalanches, which is simply related to the high-frequency part of the power-spectrum, $\mathcal{P}_{\text{av}}(\omega)$. The time-time correlation function is defined as

$$G(\theta) = \int V(t)V(t + \theta) dt. \tag{8}$$

If we assume that the magnetic field is increased adiabatically and the avalanches are well separated in time, we can calculate the time-time correlation function separately for each avalanche and then add the individual functions together to get the overall time-time correlation function.²⁴

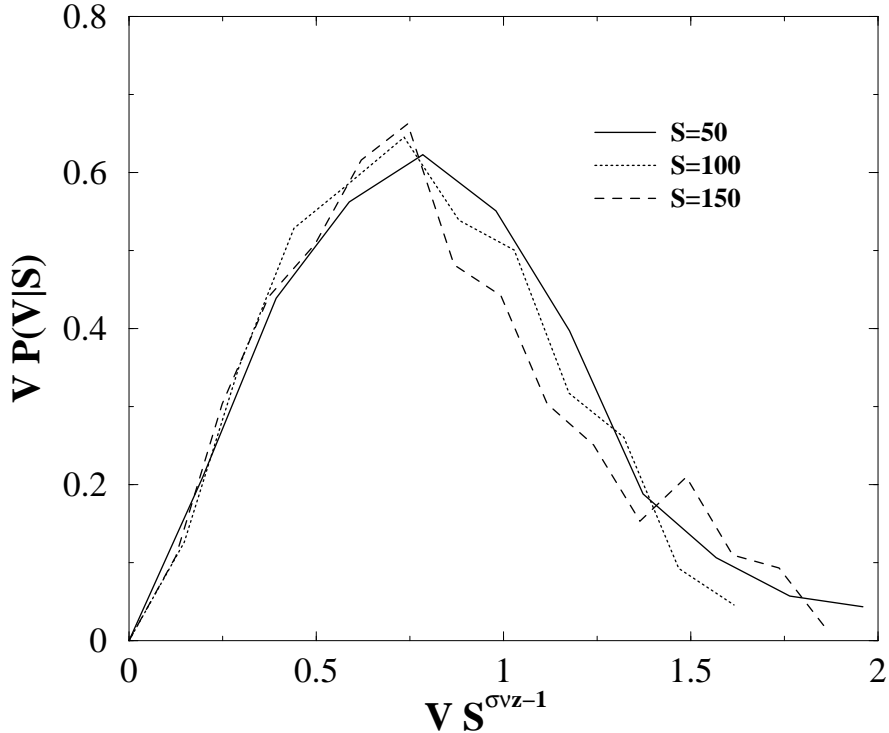


FIG. 3: A collapse of the voltage distribution for three avalanche sizes according to equation 6.

This allows us to break up the time-time correlation function into the contributions from avalanches of different sizes, S . Let $G(\theta|S)$ be the average time-time correlation function of an avalanche, *given* that the avalanche is of size S . (In contrast, the notation $G(\theta, S)$ would denote the contribution of all avalanches of size S to $G(\theta)$. This would be weighted by the probability that an avalanche is of size S , $S^{-\tau}$.) If we consider equation 8 at $\theta = 0$, we see that the $\theta = 0$ component of the correlation function is $\int V(t)^2 dt$, which is proportional to the avalanche energy. Using this fact along with the scaling of the energy from equation 7, we find that the time-time correlation function should scale as

$$G(\theta|S) = S^{2-\sigma_{VZ}} f(\theta S^{-\sigma_{VZ}}). \quad (9)$$

As shown in figure 4, this scaling works very well over a wide range of avalanche sizes.

E. The scaling of the energy spectrum with S

The energy spectrum describes the amount of energy released in Barkhausen noise at each frequency. It can be calculated as the cosine transform of the time-time correlation function. Transforming equation 9, we find that the scaling of the energy spectrum with avalanche size has the form

$$\begin{aligned} E(\omega|S) &= \int_0^\infty \cos(\omega\theta) G(\theta|S) d\theta \\ &= \int_0^\infty \cos(\omega\theta) S^{2-\sigma_{VZ}} f(\theta S^{-\sigma_{VZ}}) d\theta \\ &= S^2 f(\omega^{1/\sigma_{VZ}} S). \end{aligned} \quad (10)$$

A collapse of the energy spectra for different avalanche sizes according to this form is shown in figure 5.

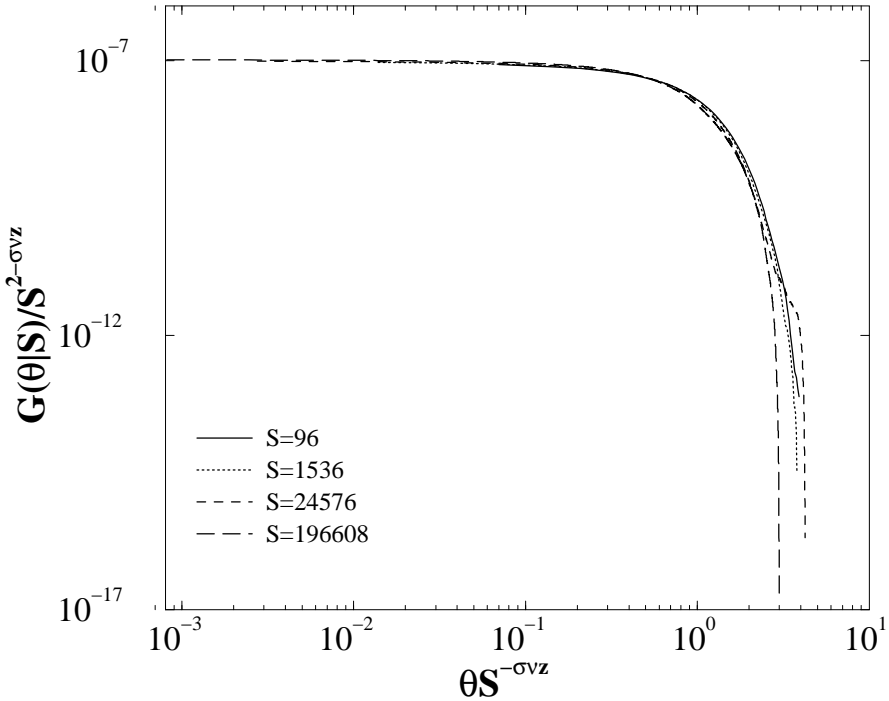


FIG. 4: A collapse of avalanche time-time correlation functions according to equation 9. The data is binned logarithmically to get good statistics.

F. The cutoff in the energy spectrum doesn't scale

The energy spectrum for all avalanches (the quantity usually measured in experiments) is just the integral $\int P(S)E(\omega|S)dS$, where $P(S) \sim S^{-\tau}$ is the probability that an avalanche will be of size S . Unfortunately, however, we can not just naively integrate equation 10. As seen in figure 5, the high frequency cutoffs don't scale in a universal way. In fact, for the models described in this paper, the high frequency cutoff is always at the same value of ω . This constant high-frequency cutoff is a simple result of the fact that there is a minimum time scale in the problem due to the finite duration of each shell in the avalanche. In section III H we will see that this has important implications for the integral over avalanche sizes, and hence for the form of the energy spectrum.

It is also apparent from figure 5 that except for the fixed high ω cutoff and a small region at small ω , the energy spectrum is a pure power law. This means that we can approximate the power spectrum as a pure power law with a fixed high omega cutoff and a small ω cutoff which scales according to equation 10. We shall argue in section III G that except at very small frequencies the energy at a fixed frequency ω is proportional to S . According to equation 10, this implies that the power spectrum at fixed S scales as $\omega^{-1/\sigma\nu z}$. This means that dividing $E(\omega|S)$ by $S\omega^{-1/\sigma\nu z}$ should collapse the curves and eliminate the ω dependence. Since the x-axis is not rescaled, the fixed high ω cutoffs should also be correctly collapsed by this form. The result of this collapse for the infinite-range model can be seen in figure 6.

G. Why does the energy at frequency ω scale linearly with the avalanche size S ?

The fact that the energy at frequency ω scales linearly with S follows from two assumptions. First, each spin in the avalanche contributes equally to $E(\omega)$. Second, the contribution of a given spin is independent of the size of the avalanche it is in. (Of course, a few spins at the beginning of the avalanche might differ, so long as the fraction of such spins vanishes for large avalanches.) One way in which this could be true would be if the following two hypotheses were true. First, each spin contributes to $E(\omega)$ only through its correlations with physically nearby spins. Second, the local growth of an avalanche does not reflect the overall size of the avalanche. The first hypothesis seems likely in the models described in this paper because the times of physically distant spin flips are likely to be randomly distributed in time and contribute incoherently to the power spectrum. Only nearby spin flips will be correlated in time and

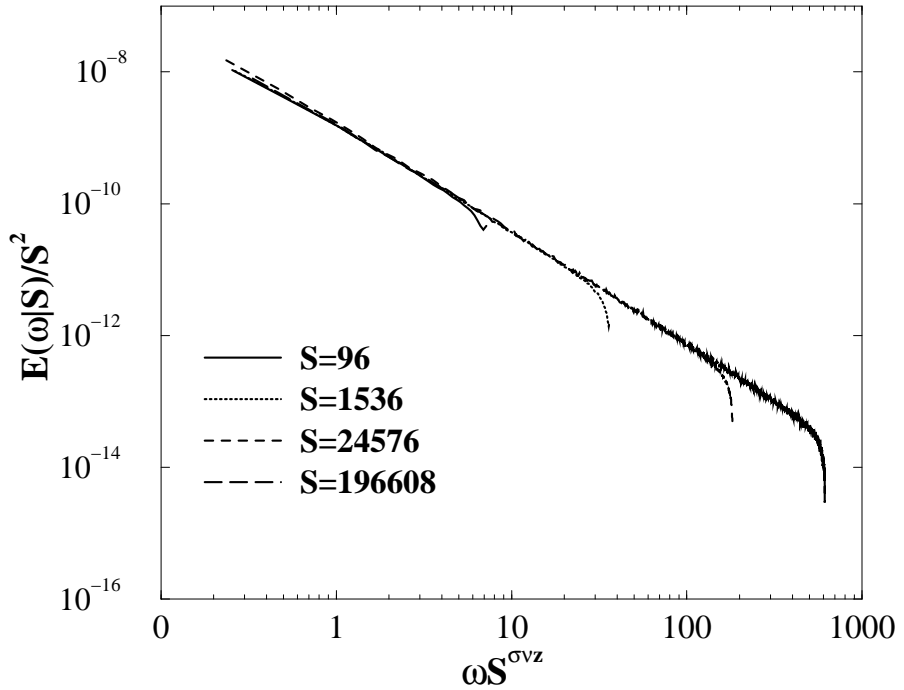


FIG. 5: A collapse of the energy spectra for different avalanche sizes according to equation 10.

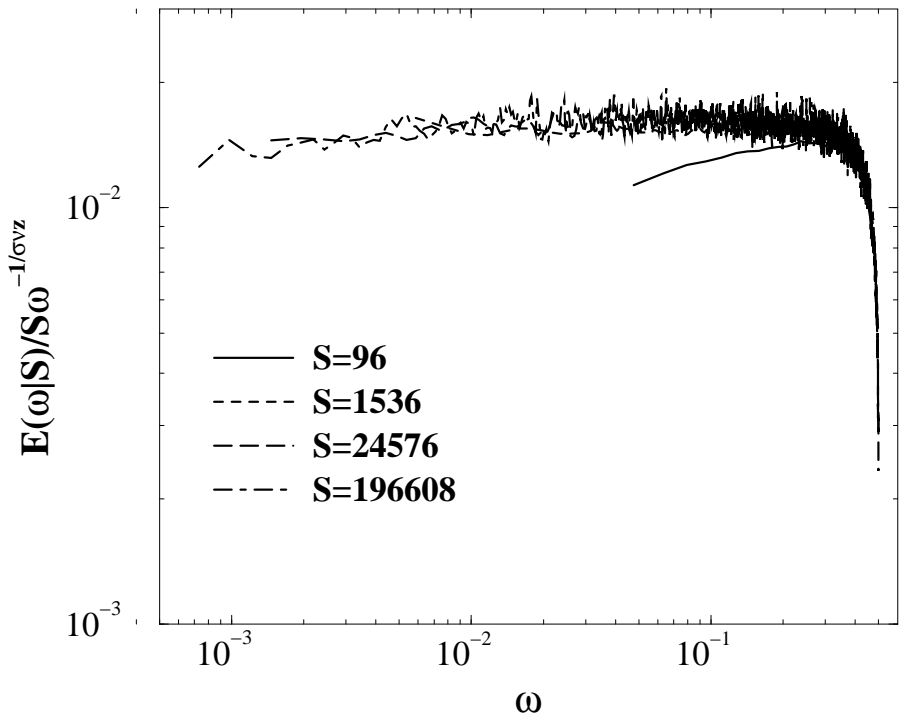


FIG. 6: A collapse of the energy spectra for several avalanche sizes S . The collapse is performed by dividing out the linear S dependence. The curves are made flat by dividing out the simple power law $\omega^{1/\sigma\nu z}$. The ω axis has not been rescaled, so the high ω cutoffs collapse together and the small ω cutoffs do not.

contribute coherently. The second hypothesis is also likely to be true because the avalanches are occurring at a critical point. Every part of the avalanche is always on the verge of stopping regardless of the size of the avalanche.

We can check these hypotheses by breaking up the energy spectrum into the contributions from pairs of spins at different radii r . The time-time correlation function for avalanches of size S can be written in terms of individual pairs of spins as

$$G(\theta|S) = \sum_{i,j} \delta(t_j - t_i - \theta), \quad (11)$$

where t_i is the time at which spin i flips. From this form, we can use an additional delta function to pull out the contribution due to pairs of spins separated by a distance r :

$$G(\theta, r|S) = \left\langle \sum_j \delta(t_j - t_i - \theta) \delta(|\vec{r}_j - \vec{r}_i| - r) \right\rangle_i, \quad (12)$$

where $\langle \rangle_i$ implies an averaging over all values of i . Using this definition of the function $G(\theta, r|S)$, we can rewrite the time-time correlation function as

$$G(\theta|S) = S \int G(\theta, r|S) dr. \quad (13)$$

Now, we can use equation 13 to calculate the contribution of spins separated by a distance r to the energy spectrum $E(\omega|S)$ at a frequency ω . Taking the cosine transform of equation 13, we find that

$$\begin{aligned} E(\omega|S) &= S \int \int \cos(\omega\theta) G(\theta, r|S) dr d\theta \\ &\equiv S \int E(\omega, r|S) dr, \end{aligned} \quad (14)$$

where the function $E(\omega, r|S)$ is defined by this equation. Notice that $E(\omega, r|S)$ must have a cutoff at the largest r present in an avalanche of size S . We can see from equation 14 that in order for $E(\omega|S)$ to be proportional to S , the integral must be independent of this S dependent cutoff. This is a more precise statement of the hypothesis that only correlations between nearby spins contribute to the energy spectrum. It is also necessary that except for extreme values of ω and r , $E(\omega, r|S)$ must be independent of S . Combined with the first condition, this corresponds to the hypothesis that the local growth of the avalanche should not reflect the overall size of the avalanche.

Figure 7 shows that the decay of $E(\omega, r|S)$ is decaying approximately as $1/r$. Figure 8 shows that it is independent of S and that the decay is oscillating about zero. Neighboring radial shells contribute with opposite sign. Hence the integral 14 appears to be conditionally convergent at large distances: each spin contributes to $E(\omega)$ only through its correlations with nearby spins, and $E(\omega|S) \sim S$.

H. Integrating the energy spectrum over avalanche sizes

We are now ready to integrate the energy spectrum over S . In order to get a convergent integral, we cut off the integral for avalanches of size $S > S^*$. In our simulations this cutoff results primarily from finite size effects ($S^* \sim L^{1/\nu}$). In experiments, it could also arise from a finite experimental duration or from the demagnetizing forces. (In some cases, demagnetizing forces also contribute to the cutoff in our simulations.) For ease in performing the integral, we assume the universal cutoff at small ω is a sharp one, but any rapid cutoff with the proper scaling leads to the same scaling result. With these approximations, the integral becomes

$$\begin{aligned} E(\omega) &= \int_{\omega^{-1/\sigma\nu z}}^{S^*} P(S) S \omega^{-1/\sigma\nu z} dS \\ &= \int_{\omega^{-1/\sigma\nu z}}^{S^*} S^{1-\tau} \omega^{-1/\sigma\nu z} \\ &= (S^*)^{2-\tau} \omega^{-1/\sigma\nu z} - \omega^{(3-\tau)/\sigma\nu z}. \end{aligned} \quad (15)$$

The energy spectrum should be proportional to the total time and the total size of the experiment. Thus the growth with the cutoff S^* is expected. Experiments usually actually measure the power spectrum, in which the total time

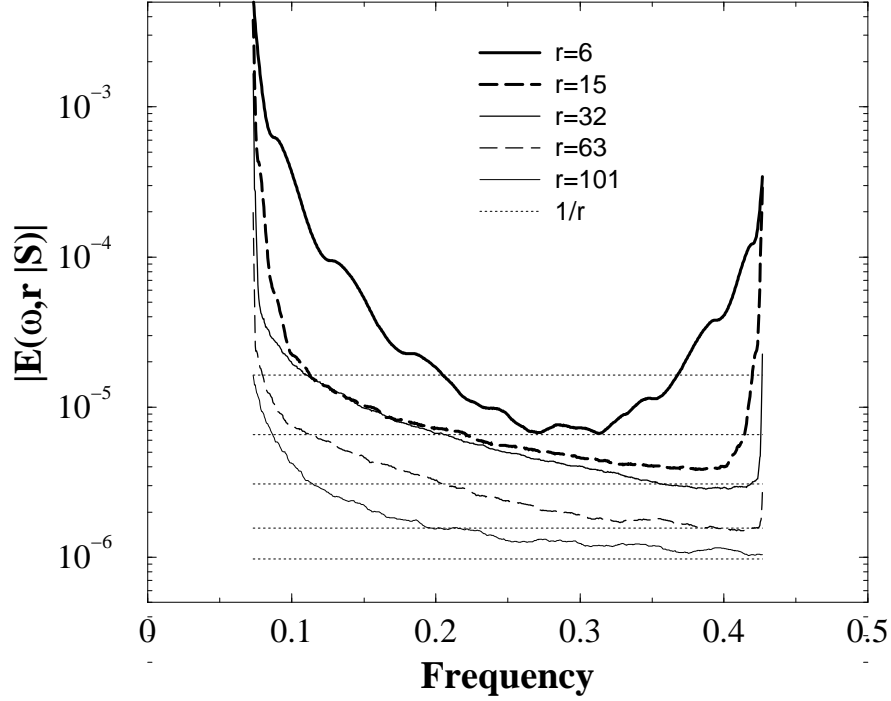


FIG. 7: This graph shows the function $|E(\omega, r | S)|$ for a range of values of r at $S = 32500$. The function $E(\omega, r | S)$ not only decays with ω , but also oscillates about zero. To better compare the amplitudes of the curves at different r , we took the absolute value and performed a running average over ω , averaging out the oscillations. The horizontal lines show how the positions of these curves should scale if they went as $1/r$. Notice that while for small r the amplitudes drop slower than $1/r$, for larger r the amplitudes drop off approximately as $1/r$.

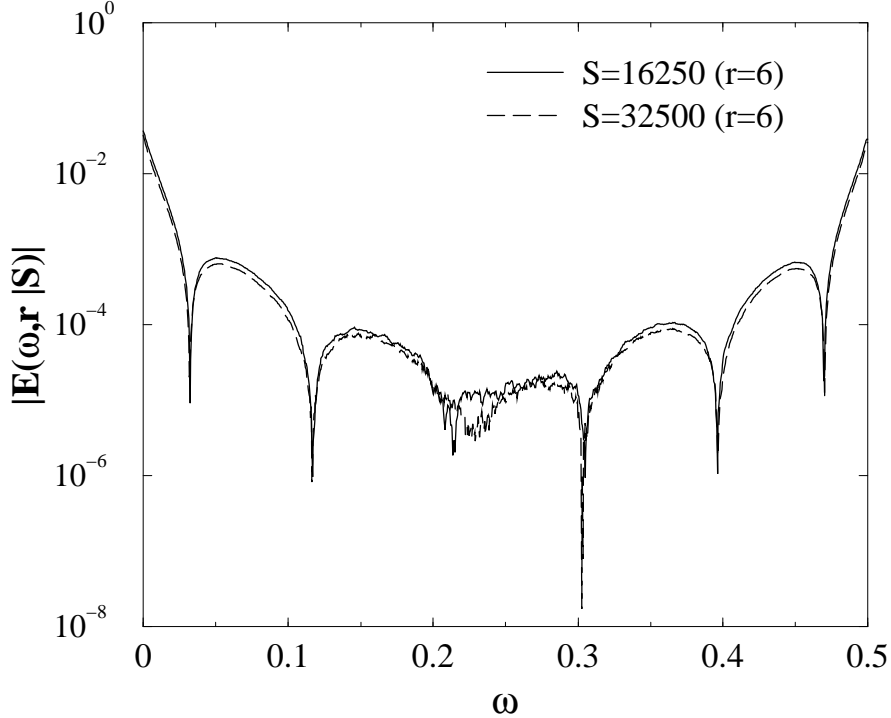


FIG. 8: This graph shows $|E(\omega, r | S)|$ at $r = 6$ for two sizes of avalanches. No averaging has been performed, so the oscillations are visible (the function changes sign at each dip). For larger r , the oscillations are much faster. Notice that the curves are nearly identical for the two sizes— $E(\omega, r | S)$ has no significant S dependence at small r .

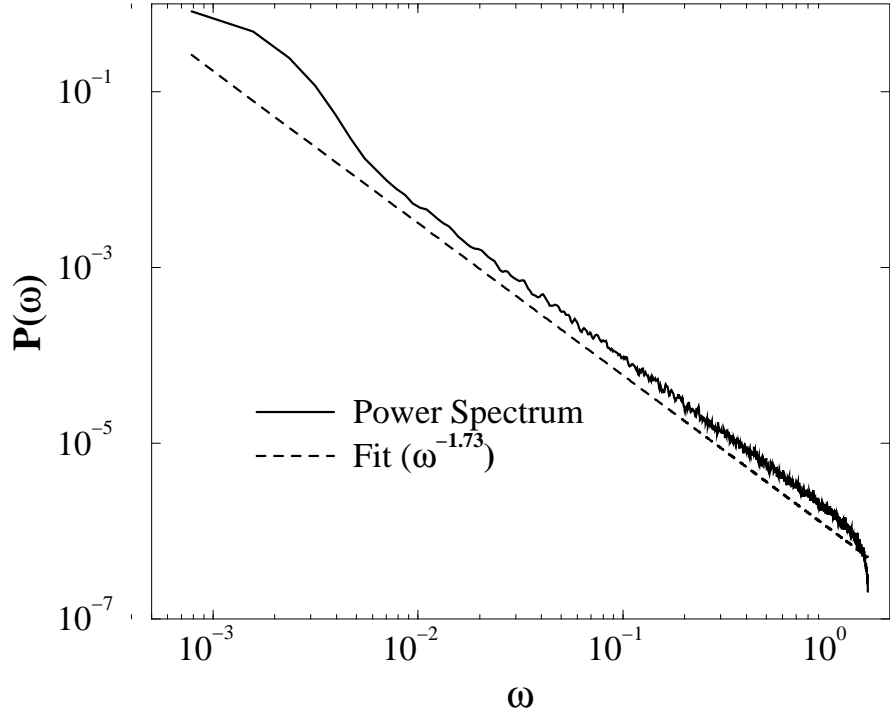


FIG. 9: The power spectrum for the infinite range model. The dashed line is not a fit. It is a power law with an exponent $1/\sigma\nu z$.

	$1/\sigma\nu z$	$(3 - \tau)/\sigma\nu z$	Simulated
Short-range	1.72	2.41	1.70
Infinite-range	1.72	3.00	1.70
Dipole	2.00	3.00	2.00

TABLE II: This table compares values of the power spectrum exponent measured in simulations with the values predicted by the exponents $1/\sigma\nu z$ and $(3 - \tau)/\sigma\nu z$. Notice that for all three models $1/\sigma\nu z$ is very close to the simulated exponent, and $(3 - \tau)/\sigma\nu z$ is in complete disagreement.

T^* has been divided out. Dividing out this factor, we find that the power spectrum is

$$\mathcal{P}(\omega) = \frac{(S^*)^{2-\tau}}{T^*} \omega^{-1/\sigma\nu z} - \frac{1}{T^*} \omega^{(3-\tau)/\sigma\nu z}. \quad (16)$$

If the cutoff S^* is entirely due to a finite duration of the simulation, then T^* will be equal to $(S^*)^{2-\tau}$ and the first term will be independent of T^* .

The exponent in the second term of equation 16, $(3 - \tau)/\sigma\nu z$, is the power that was predicted by Dahmen and Sethna^{5,8,9} and Spasojević *et al.*¹². This is indeed the result we would get if we ignored the fact that the high ω cutoff does not scale. However, as we can see in equation 16, for $\tau < 2$ the first term will dominate over the second term both for large system sizes and for large ω . Only for $\tau > 2$ will the second term will dominate. For all of the models we are considering, $\tau < 2$. (See table I) In fact, the exponent $(3 - \tau)/\sigma\nu z$ disagrees badly with the results observed in both simulations and experiments, and the exponent $1/\sigma\nu z$ agrees very well. In mean field theory, we can actually derive rigorously that the power spectrum exponent is 2 (see appendix A). This is in perfect agreement with the exponent $1/\sigma\nu z$, and complete disagreement with the exponent $(3 - \tau)/\sigma\nu z$, which would be 3. A plot of the power law for the infinite-range model can be seen in figure 9. A comparison of the two possible exponents with simulations for each of the three models can be seen in table II.

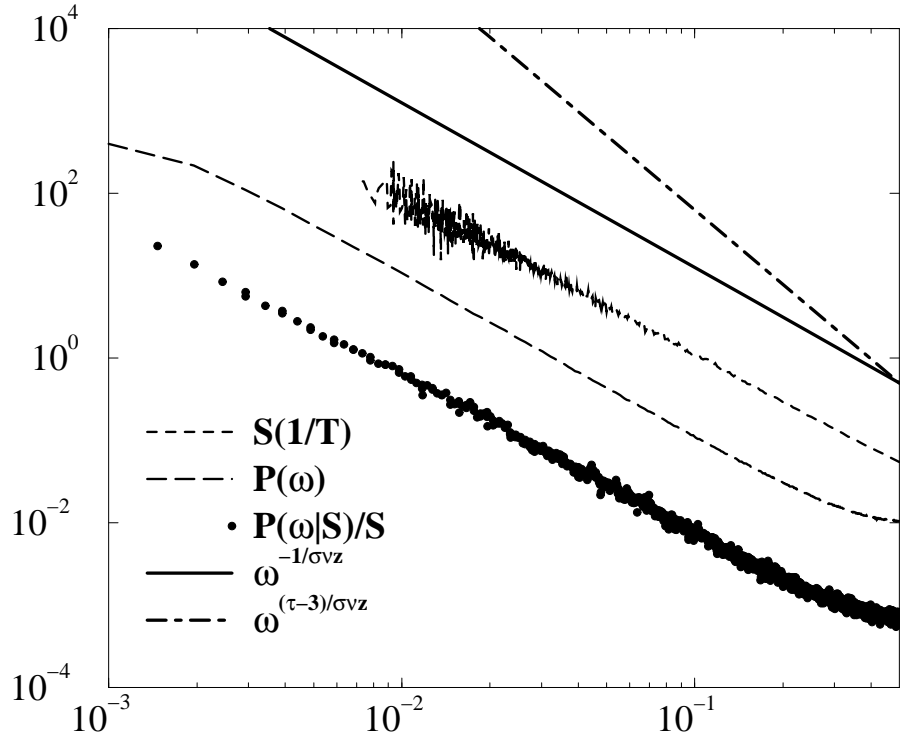


FIG. 10: The mean field model. Notice that the energy spectrum for avalanches of size S collapses when divided by S , and that the energy spectrum for avalanches of size S and the overall energy spectrum both have the same power law as the average avalanche size as a function of the inverse avalanche duration. Sizes 96, 1536, 24576, and 196608 are shown in the collapse of $P(\omega|S)/S$. The average avalanche size as a function of the inverse avalanche duration is the definition of the exponent $1/\sigma\nu z$. Power laws of $1/\sigma\nu z$ and $(3 - \tau)/\sigma\nu z$ are also shown for comparison. Notice that $(3 - \tau)/\sigma\nu z$ is completely incompatible with the results.

IV. HOW UNIVERSAL IS THE EXPONENT $1/\sigma\nu z$?

We have shown quite generally that the non-universal scaling of the high ω cutoff in $E(\omega|S)$ causes the naive exponent of $(3 - \tau)/\sigma\nu z$ to be incorrect whenever $\omega^{(3-\tau)/\sigma\nu z}$ decays more rapidly than $E(\omega|S)$. (In our models, where we have shown that $E(\omega|S) \sim \omega^{-1/\sigma\nu z}$, this occurs for all $\tau < 2$.) Instead, the exponent of the overall energy spectrum $E(\omega)$ is the same as the exponent for the energy spectrum for avalanches of a fixed size S , $E(\omega|S)$. However, the conclusion that the exponent for the energy spectrum at fixed S was $1/\sigma\nu z$ was based on less general arguments. In fact, for models with very different dynamics, it is likely that the exponent will not be $1/\sigma\nu z$.

So far, we have only verified these results for the infinite range model in three dimensions. However, we have also checked these results in several other situations where both τ and $\sigma\nu z$ take on a range of values. (In all cases, $\tau < 2$.) We have checked the short-range model in 3 and 4 dimensions, the infinite-range model in 3 and 4 dimensions, and mean field theory. In all cases, the linear scaling with S seems exact, and both $E(\omega|S)$ and $E(\omega)$ scale as $\omega^{-1/\sigma\nu z}$ to within simulational precision. In all cases, the exponent $(3 - \tau)/\sigma\nu z$ is completely inconsistent with the observed results. The results of mean field theory and the short-range model at the three dimensional critical point can be seen in figures 10 and 11. The results for the four dimensional short-range model and the four dimensional infinite range model were also completely consistent with a $1/\sigma\nu z$ scaling exponent.

V. DISCUSSION

There have been several previous predictions of the power spectrum exponent. In her Ph.D. thesis, Karin Dahmen⁹ did a calculation similar to the one done in this paper, but she ignored the problems with the integral and came up with the exponent $(3 - \tau)/\sigma\nu z$. This exponent was published by our group⁵ without any derivation, and was compared to experimental work by Cote and Meisel^{16,17} and Bertotti *et al.*¹⁸ The correct exponent form derived here makes the agreement between the short-range model and these experiments substantially better: they quote an exponent of “around 2”, our former (wrong) prediction was 2.46 ± 0.17 , and the correct prediction is 1.75 ± 0.25 .

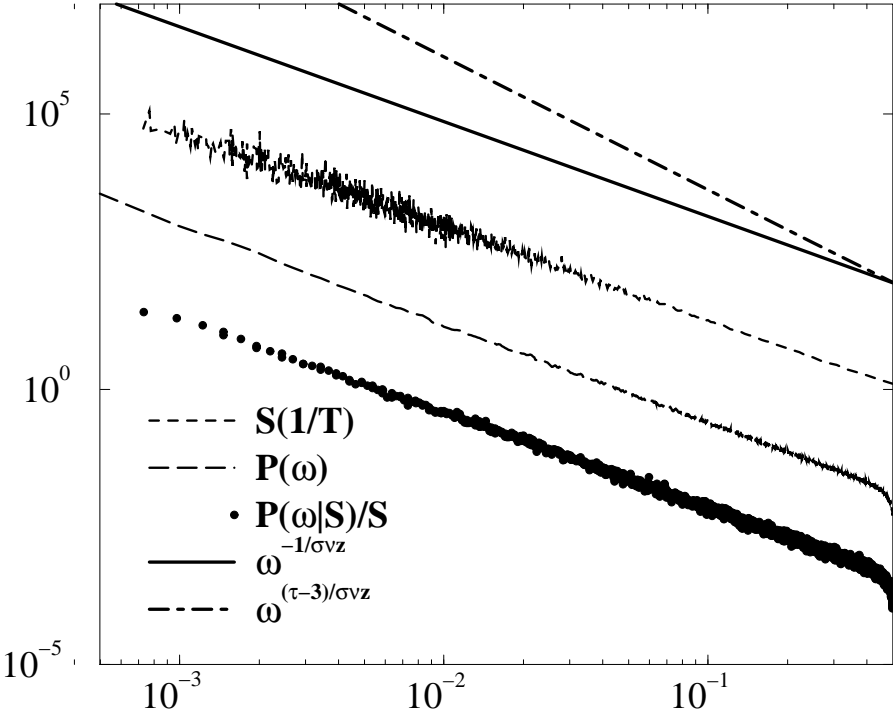


FIG. 11: The short-range model in 3 dimensions. The plots and the sizes are the same as in figure 10.

Spasojević, Bukvić, Milosević and Stanley¹² also came up with the same (wrong) form based on arguments about the average pulse shape. They measured an experimental power spectrum exponent of 1.6. For their experimentally determined values of $\tau = 1.77$ and $\sigma\nu z = 0.662$, they found that $(3 - \tau)/\sigma\nu z = 1.86$ fit their data well, but the value of $(3 - \tau)/\sigma\nu z = 2.46$ quoted by Dahmen *et. al.*⁵ was much too large. This lead them to disregard the plain old critical model with domain nucleation as a possible explanation of Barkhausen noise in their system. However, note that their experimental value of $1/\sigma\nu z = 1.51$ is as close to their measured power spectrum exponent as their value of $(3 - \tau)/\sigma\nu z = 1.86$. The value of $1/\sigma\nu z = 1.75 \pm 0.25$ quoted by Dahmen *et. al.* is even closer to the experimentally observed power spectrum exponent. The value of $\tau = 1.6$ predicted by Dahmen *et. al.* is also closer to the experimentally measured $\tau = 1.77$ than any of the other models. (Front propagation has an exponent $\tau = 1.3$, and mean-field theory has an exponent $\tau = 1.5$.) One should note, however, that the average avalanche shapes measured by Spasojević *et. al.* disagree with those predicted by the short-range model (figure 2).

In 1989, Jensen, Christensen and Fogedby¹⁹ published a different calculation of the power spectrum exponent for sandpile models, which has been cited many times as an explanation for $1/\omega^2$ scaling of the power spectrum in sandpiles, Barkhausen noise, and other systems. They made two major assumptions in their derivation. First, they assumed that the avalanche shape could be approximated by a box function: $V(t) = S/T$ for all $t < T$. For our models, this assumption turns out to be valid for calculating the average avalanche energy, but is not valid for determining the overall scaling of the time-time correlation function. Second, they assumed that one of their scaling functions, which was related to the time-time correlation function, had the simple scaling form $G(T) \sim T^\alpha \exp(-T/T_0)$. As can be seen from the exact mean field time-time correlation function in equation A6, this is not at all a safe assumption. In terms of our exponents τ and $\sigma\nu z$, their prediction was that the energy spectrum would have the form $E(\omega) \sim \omega^{(3-\tau)/\sigma\nu z}$ for $\tau > 3 - 2\sigma\nu z$ and $E(\omega) \sim \omega^{-2}$ for $\tau < 3 - 2\sigma\nu z$. This is the same as our result in the case where $\sigma\nu z = 1/2$. For the particular model they were studying, their assumptions seem to be correct, but in the more general case, the exponent $(3 - \tau)/\sigma\nu z$ should become invalid for $\tau < 2$, rather than $\tau < 3 - \sigma\nu z$. Also, for $\tau < 2$, exponents other than 2 are possible, depending on the particular dynamics. For the class of models described in this paper, the correct exponent for $\tau < 2$ is $1/\sigma\nu z$.

There are other specific models for which the power spectrum exponent has been calculated. For example, Bak, Tang and Wiesenfeld² calculated the power spectrum exponent for their sandpile models. Without further investigation, we can't expect our arguments for an exponent of $1/\sigma\nu z$ to hold for these and other models. However we do expect that in any avalanche based model, the power spectrum exponent for $\tau > 2$ will be $(3 - \tau)/\sigma\nu z$, and another exponent will dominate for $\tau < 2$. Whenever the arguments in section III G hold, we expect that for $\tau < 2$ the exponent $1/\sigma\nu z$ will dominate. (Where $1/\sigma\nu z$ is the exponent relating avalanche size to avalanche duration.)

APPENDIX A: THE MEAN FIELD POWER SPECTRUM

In mean field theory, we can calculate the power spectrum exactly. The Hamiltonian in mean field theory is the Hamiltonian in equation 1, without nearest neighbor or dipole terms:

$$\mathcal{H} = - \sum_i (H + J + h_i) s_i. \quad (\text{A1})$$

When a spin flips with an external field of H , all spins with random fields between $-(H+JM)$ and $-(H+J(M+2/N))$ will flip. Therefore, each spin has a probability of $\frac{2J}{N}\rho(-H-JM)$ of flipping, where $\rho(h)$ is the probability distribution of the random fields. On average, $2J\rho(-H-JM)$ spins will be flipped. If $2J\rho(-H-JM) > 1$, then the avalanche will tend to grow indefinitely, and there will be an infinite avalanche. If $2J\rho(-H-JM) < 1$, then the avalanche will quickly die out, and all avalanches will be small. If $2J\rho(-H-JM) = 1$, then avalanches will always be finely balanced between continuing and dying, and there will be a critical distribution of avalanches. If the random field distribution $\rho(h)$ has a maximum value of $1/2J$, then there will be a critical distribution of avalanches at the value of $H = H_c$ where $\rho(h)$ is a maximum.

Let us calculate the power spectrum for the critical system with $\rho(h) = 1/2J$. To begin with, we will calculate the probability distribution of time-series $n_1, n_2, \dots, n_\infty$. We know that in shell zero, exactly $n_0 = 1$ spins will flip. At the critical point, where each spin on average causes one more spin to flip, shell one will have a Poisson distribution with mean one: $P(n_1) = \frac{1}{en_1!}$. Shell i will have a Poisson distribution with mean n_{i-1} : $P(n_i) = \frac{e^{n_{i-1}} n_{i-1}^{n_i}}{n_i!}$. Therefore, the probability distribution for the entire time series will be

$$P(1, n_1, n_2, \dots, n_\infty) = \frac{1}{en_1!} \prod_{i=2}^{\infty} \frac{e^{n_{i-1}} n_{i-1}^{n_i}}{n_i!}. \quad (\text{A2})$$

Now, from equation A2, we can calculate the average time-time correlation function

$$G(\theta) = \sum_{i=0}^{\infty} \langle n_i n_{i+\theta} \rangle, \quad (\text{A3})$$

where

$$\langle n_i n_{i+\theta} \rangle = \sum_{\{n_1, \dots, n_\infty\}=0} n_i n_{i+\theta} P(n_1, \dots, n_\infty). \quad (\text{A4})$$

To simplify equation A4, we need to use several properties of the Poisson distribution: $\sum_{n=0}^{\infty} \frac{e^{-x} x^n}{n!} = 1$, $\sum_{n=0}^{\infty} n \frac{e^{-x} x^n}{n!} = x$, and $\sum_{n=0}^{\infty} n^2 \frac{e^{-x} x^n}{n!} = x + x^2$. Using the first rule repeatedly, we can simplify equation A4 to

$$\langle n_i n_{i+\theta} \rangle = \sum_{\{n_1, \dots, n_{i+\theta}\}=0} n_i n_{i+\theta} P(n_1, \dots, n_{i+\theta}).$$

Then, using the second rule repeatedly, we can further simplify to

$$\langle n_i n_{i+\theta} \rangle = \sum_{\{n_1, \dots, n_i\}=0}^{\infty} n_i^2 P(n_1, \dots, n_i).$$

Now, applying the second and third rules repeatedly, we can simplify to a single sum:

$$\begin{aligned} \langle n_i n_{i+\theta} \rangle &= \sum_{n_1=0}^{\infty} \frac{(i-1)n_1 + n_1^2}{en_1!} \\ &= i + 1. \end{aligned} \quad (\text{A5})$$

Notice that the correlation between two times is proportional only to the first time, and not the separation between the times.

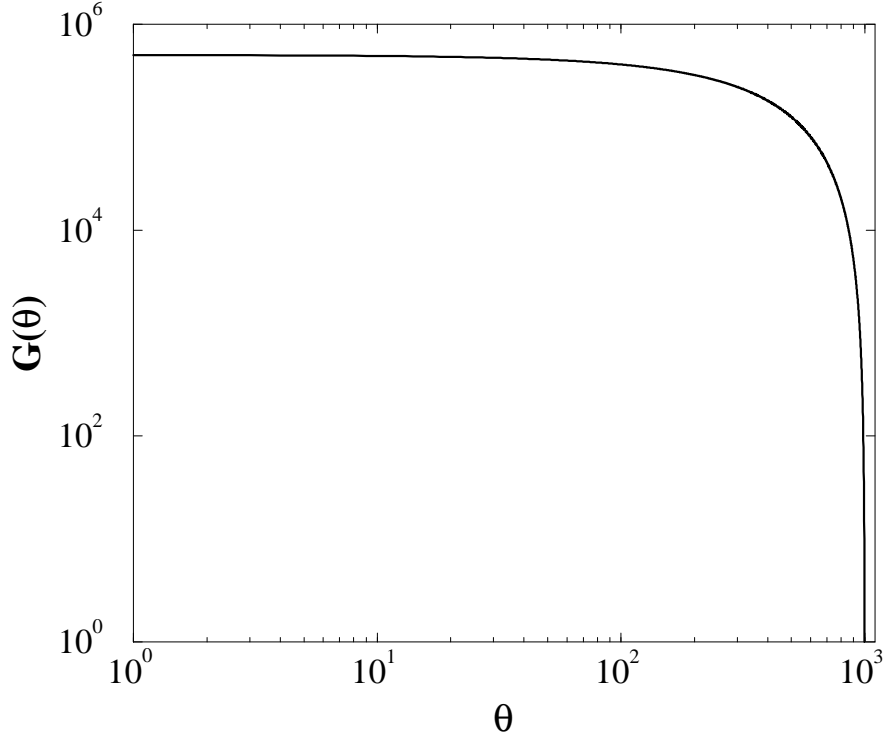


FIG. 12: The exact time-time correlation for mean field theory with a maximum time cutoff of $T = 1000$.

Now, we can find the value of the time-time correlation function $G(\theta)$ by summing the result of equation A5. Because the time-time correlation function as defined is proportional to the square of the total time, we must cut off the summation at some maximum time T to get a finite result. Summing according to equation A3, we find

$$\begin{aligned}
 G(\theta) &= \sum_{i=0}^{T-\theta-1} i + 1 \\
 &= \frac{(T-\theta)(T-\theta+1)}{2} \\
 &= \frac{T^2}{2} + \frac{T}{2} + \frac{\theta^2}{2} - \frac{\theta}{2} - T\theta.
 \end{aligned} \tag{A6}$$

This shape for a cutoff time of $T = 1000$ is shown in figure 12. Notice that the exact shape in mean-field theory is very similar to the experimentally measured correlation functions in three dimensions.

To get the exact form of the mean-field energy spectrum, we just take the cosine transform of equation A6.

$$\begin{aligned}
 E(\omega) &= \int_0^\infty \cos(\omega\theta)G(\theta)d\theta \\
 &= \int_0^\infty \cos(\omega\theta) \left(\frac{T^2}{2} + \frac{T}{2} + \frac{\theta^2}{2} - \frac{\theta}{2} - T\theta \right) d\theta \\
 &= T\omega^{-2} + \frac{\omega^{-2}}{2}(1 - \cos(T\omega)) - \omega^{-3} \sin(T\omega).
 \end{aligned} \tag{A7}$$

The dominant term in this equation is $T\omega^{-2}$. This is the same exponent as predicted by the general scaling arguments: $\frac{1}{\sigma\nu z} = 2$. The general scaling arguments also predicted that a term smaller by a factor of T and with the exponent $(3-\tau)/\sigma\nu z = 3$ would be subtracted off, and it is, but multiplied by a factor of $\sin(T\omega)$. However, the $\sin(T\omega)$ turns out to simplify things even more. Because the correlation function was actually discrete, we should consider a discrete power spectrum, where the frequencies are multiples of $\omega_0 = \frac{2\pi}{T}$. This means that $\cos(T\omega) = 1$ and $\sin(T\omega) = 0$ for all ω in the discrete spectrum. Because of this, all terms except the $T\omega^{-2}$ term drop out. If we divide by T to get

the power spectrum, we find

$$\mathcal{P}(\omega) = \omega^{-2}. \quad (\text{A8})$$

* mck10@cornell.edu

† sethna@lassp.cornell.edu

- ¹ S. Field, J. Witt, F. Nori, and X. Ling, Phys. Rev. Lett. **74**(7), 1206 (February 13 1995).
- ² P. Bak, C. Tang, and K. Wiesenfeld, Phys. Rev. A **38**(1), 364 (July 1 1998).
- ³ E. Vives, J. Ortín, L. Mañoso, I. Ràfols, and R. Pérez-Magrané, Phys. Rev. Lett. **72**(11), 1694 (March 14 1994).
- ⁴ J. P. Sethna, K. Dahmen, S. Kartha, J. A. Krumhansl, B. W. Roberts, and J. D. Shore, Phys. Rev. Lett. **70**(21), 3347 (May 24 1993).
- ⁵ O. Perković, K. A. Dahmen, and J. P. Sethna, Phys. Rev. Lett. **75**(24), 4528 (December 11 1995).
- ⁶ O. Perković, K. A. Dahmen, and J. P. Sethna, *Disorder-induced critical phenomena in hysteresis: A numerical scaling analysis*, cond-mat #9609072, Los Alamos Nat'l Laboratory, Los Alamos, N. M.; <http://xxx.lanl.gov/abs/cond-mat/9609072>.
- ⁷ O. Perković, K. A. Dahmen, and J. P. Sethna, *Disorder-induced critical phenomena in hysteresis: Numerical scaling in three and higher dimensions*, cond-mat #9807336, Los Alamos Nat'l Laboratory, Los Alamos, N. M.; <http://xxx.lanl.gov/abs/cond-mat/9807336>.
- ⁸ K. A. Dahmen and J. P. Sethna, Phys. Rev. B. **53**(22), 14872 (June 1996).
- ⁹ K. A. Dahmen, *Hysteresis, Avalanches, and Disorder Induced Critical Scaling: A Renormalization Group Approach*, Ph.D. thesis, Cornell University (May 1995).
- ¹⁰ J. S. Urbach, R. C. Madison, and J. T. Markert, Phys. Rev. Lett. **75**(2), 276 (July 10 1995).
- ¹¹ S. Zapperi, P. Cizeau, G. Durin, and H. E. Stanley, Phys. Rev. B **58**(10), 6353 (September 1 1998).
- ¹² D. Spasojević, S. Bukvić, S. Milosević, and H. E. Stanley, Phys. Rev. E **54**(3), 2531 (September 1996).
- ¹³ M. C. Kuntz, *Universality in barkhausen noise: Simulation and experiment*, unpublished.
- ¹⁴ H. Ji and M. O. Robbins, Phys. Rev. B **46**(22), 14519 (September 1992).
- ¹⁵ O. Narayan, Phys. Rev. Lett. **77**(18), 3855 (October 28 1996).
- ¹⁶ P. J. Cote and L. V. Meisel, Phys. Rev. Lett. **67**(10), 1334 (Sept 1991).
- ¹⁷ L. V. Meisel and P. J. Cote, Phys. Rev. B **46**(17), 10822 (Nov 1992).
- ¹⁸ G. Bertotti, F. Fiorillo, and A. Montorsi, J. Appl. Phys. **67**(9), 5574 (May 1990).
- ¹⁹ H. J. Jensen, K. Christensen, and H. C. Fogedby, Phys. Rev. B **40**(10), 7425 (October 1 1989).
- ²⁰ This is not the same as a mean-field model, because the model contains nearest neighbor interactions along with the infinite range interactions.
- ²¹ The non-self-organized scaling described by Ji and Robbins also occurs below R_c in the model of Sethna *et al.* with domain nucleation. Below R_c with domain nucleation, the front sees some preflipped regions ahead which act as a second source of random, correlated disorder. However, below R_c these regions typically have a small radius given by the correlation length $\xi \sim ((R_c - R)/(R_c))^{-\nu}$. On a scale large compared to the correlation length the behavior is still well described by the front propagation model of Ji and Robbins.
- ²² In earlier papers^{4,5,6,7,8}, our group has called the exponent relating avalanche size to avalanche duration $\sigma\nu z$. σ is the exponent describing the growth of the cutoff in the avalanche size distribution with increasing disorder. ν is the exponent describing the growth of the correlation function as the critical disorder is approached. z describes the dynamics of the model.
- ²³ This shape is very well fit by an inverted parabola. In mean field theory, this fit seems to be exact.
- ²⁴ There should also be contributions from cross-terms between avalanches, but this will contribute only at a time θ which grows as the field is ramped more and more slowly. In the limit of an adiabatically slowly increasing field, these cross terms will affect only the $\omega = 0$ scaling of the power spectrum. Here, we are calculating the scaling behavior for large ω .